

This is the accepted manuscript made available via CHORUS. The article has been published as:

Disappearance of the Mach cone in heavy-ion collisions

Christine Nattrass, Natasha Sharma, Joel Mazer, Meghan Stuart, and Aram Bejnood

Phys. Rev. C **94**, 011901 — Published 28 July 2016

DOI: [10.1103/PhysRevC.94.011901](https://doi.org/10.1103/PhysRevC.94.011901)

Disappearance of the Mach Cone in heavy ion collisions

Christine Nattrass,¹ Natasha Sharma,^{1,2} Joel Mazer,¹ Meghan Stuart,¹ and Aram Bejnood¹

¹*University of Tennessee, Knoxville, TN, USA-37996.*

²*Department of Physics, Panjab University, Chandigarh, India-160014.*

(Dated: July 11, 2016)

We present an analysis of di-hadron correlations using recently developed methods for background subtraction which allow for higher precision measurements with fewer assumptions about the background. These studies indicate that low momentum jets interacting with the medium do not equilibrate with the medium, but rather that interactions with the medium lead to more subtle increases in their widths and fragmentation functions, consistent with observations from studies of higher momentum fully reconstructed jets. The away-side shape is not consistent with a Mach cone. The qualitatively different conclusions reached with a more careful consideration of the background subtraction call into question the complete suppression of jets in central collisions observed in earlier studies, indicating that this is also an artifact of the background subtraction.

PACS numbers: 25.75.-q, 25.75.Gz, 25.75.Bh

Keywords:

I. INTRODUCTION

A hot, dense medium called the Quark Gluon Plasma (QGP) is created in high energy heavy ion collisions [1–4]. Quarks and gluons scattered early in the collision live through the QGP phase and interact strongly with the medium. This leads to the suppression of hadrons at high transverse momenta relative to expectations from binary scaling in $p+p$ collisions [5–9], a process called jet quenching. One of the early indications of jet quenching was measurements of di-hadron correlations at high transverse momenta (p_T) [10, 11]. A high momentum particle created in an $A+A$ collision is used as a proxy for a jet, assuming that a sufficiently high p_T particle originated from a jet and that its direction is approximately the direction of the parton. The distribution of softer particles in the event, called associated particles, can be measured in azimuth ($\Delta\phi$) and pseudorapidity ($\Delta\eta$) relative to the trigger particle. The correlation function has two peaks in azimuth, one near the trigger particle ($\Delta\phi \approx 0$), called the near-side, and one 180° away, called the away-side. The near-side is roughly comparable to that observed in $d + Au$ and $p+p$ collisions, with slight modifications [12–14]. Numerous studies reported modifications of the away-side shape, observing a local minimum rather than a peak [11, 15–18]. This was frequently interpreted as a Mach cone from a parton propagating faster than the speed of sound in the QGP [19]. We refer to this as the Mach cone below. This feature indicated a qualitatively different interaction with the medium for the soft jets which dominate di-hadron correlations and the hard jets observed at the Large Hadron Collider (LHC). Studies at the LHC indicated that the fragmentation functions were slightly modified [20, 21] but studies of fully reconstructed jets have not indicated any severe shape modifications.

The combinatorial background in azimuth in di-hadron

correlations has the form

$$\frac{dN}{\pi d\Delta\phi} = B(1 + \sum_{n=2}^{\infty} 2\tilde{v}_n^t \tilde{v}_n^a \cos(n\Delta\phi)) \quad (1)$$

where \tilde{v}_n^t (\tilde{v}_n^a) are the Fourier coefficients of the trigger (associated) particles in the background [22]. The \tilde{v}_n may arise due to hydrodynamical flow or jet quenching. The majority of di-hadron correlation studies used the zero yield at minimum (ZYAM) method [23–26], or some variation thereof, to determine the background level B , combined with the assumption that independent measurements of the v_n were the appropriate \tilde{v}_n for these studies. The odd v_n were assumed to be zero until it was proposed that non-zero odd v_n could arise from fluctuations in the initial condition [27, 28]. Non-zero odd v_n were subsequently measured [29–31]. A majority of the published di-hadron correlations therefore neglect the odd v_n . While the observation of odd v_n indicated that at least the magnitude of the Mach Cone signal in the data was overestimated, theoretical studies of the Mach Cone continue [32–36]. The few di-hadron correlation studies since the observation of odd v_n are either inconclusive about the presence or absence of shape modifications [37] or indicate that the shape modification persists [38].

We reassess the data using improved background subtraction techniques in order to determine the presence or absence of shape modifications and whether or not di-hadron correlations are consistent with studies using fully reconstructed jets. In [39] we presented an alternate method for determining the background which overcomes many of the limitations of ZYAM, making fewer assumptions about the shape and level of the background. The Reaction Plane Fit (RPF) method uses the correlation functions in the background dominated region on the near-side ($\Delta\eta > 0.7$, $\Delta\phi < \pi/2$) and the fact that the \tilde{v}_n^t depend on the reaction plane when the angle of the trigger particle is restricted relative to the event plane [22]. The correlation functions in bins of the angle of the trigger particle relative to the event plane are fit simulta-

neously to determine the B , \tilde{v}_n^a , and \tilde{v}_n^t in equation 1. This method makes fewer assumptions about the shape of the background than other methods. In this paper we apply this method to di-hadron correlations before background subtraction measured by STAR [38, 40]. We briefly review the relevant details of the measurement and then present di-hadron correlations using the RPF method [39] for background subtraction.

II. ANALYSIS

In [40] correlation functions were reported for $d + Au$ collisions at $\sqrt{s_{NN}} = 200$ GeV and for 20–60% $Au + Au$ collisions at $\sqrt{s_{NN}} = 200$ GeV in bins of the angle between the trigger particle and the reconstructed reaction plane, $\phi_s = \phi^t - \psi$ in two regions in $\Delta\eta$ ($|\Delta\eta| < 0.7$ and $0.7 < |\Delta\eta| < 2.0$). The correlation functions were normalized by the number of trigger particles rather than by the number of events so all bins in ϕ_s have the same B in equation 1. The \tilde{v}_n^t in a given ϕ_s bin depend on the range of the bin in ϕ_s , the v_n^t , and the reaction plane resolution [22]. The systematic uncertainties on the reaction plane resolution were 1% for the second order reaction plane and 3% for the fourth and sixth [40].

The background is fit up to $n = 4$ in equation 1. The uncertainty due to the reaction plane resolution uncertainty is determined by varying the reaction plane resolution and refitting the background. The background determined from the background dominated region ($0.7 < |\Delta\eta| < 2.0$) must be scaled to determine the appropriate background level in the signal+background region ($|\Delta\eta| < 0.7$). The correlation functions in [40] were not corrected for acceptance effects using mixed events, as in [12, 14, 39]. If the distribution of particles in the event were independent of η , the exact scaling factor could be determined analytically, however, the η -dependent track distribution and tracking efficiency alter the ratio of the number of track pairs in the background-dominated region to the signal-dominated region. The background is scaled up by 2% more than expectations from an η -independent track distribution with a systematic error of 1%. The scale for the background is determined by comparison to the highest momentum associated momentum ($3.0 < p_T^a < 4.0$ GeV/c) and trigger momentum ($4.0 < p_T^t < 6.0$ GeV/c). The same scaling is used for all momenta. Note that the scale uncertainty is not a feature of the method and would be avoidable in future studies. The scale and reaction plane uncertainties are correlated point-to-point and when comparing correlations at different momenta. The statistical uncertainties on the $Au + Au$ data include uncertainties due to the background determined by the fit in the RPF method and are therefore non-trivially correlated point-to-point. Since the RPF method assumes that the residual signal in the background-dominated region is negligible, we restrict our study to high momenta ($4.0 < p_T^t < 6.0$ GeV/c and $1.5 < p_T^a < 4.0$ GeV/c) where PYTHIA [41, 42] stud-

ies indicate that the near- and away-side peaks are well separated. The $d + Au$ data in [40] are background subtracted and are therefore compared to the $Au + Au$ data without modification.

Fit parameters from the RPF method are given in Table I. The \tilde{v}_n^t are within error for all p_T^a and the \tilde{v}_4^t are consistent with zero. The \tilde{v}_2^a (\tilde{v}_2^t) determined from the fit are larger (smaller) than the v_2 from inclusive particles from [40]. There are several possible explanations for differences between the inclusive v_n and the \tilde{v}_n^t determined from the RPF method. The terms Equation 1 should be the weighted average of the product $\tilde{v}_n^t \tilde{v}_n^a = \langle v_n^t v_n^a \rangle$, rather than $\langle v_n^t \rangle \langle v_n^a \rangle$, and the average should be over background pairs. The centrality bin is wide and high p_T trigger particles are more likely to be in more central events, meaning that the background pair-averaged \tilde{v}_n^t in Equation 1 is not necessarily the same as the inclusive v_n . Events which contain high p_T particles may not have the same properties as inclusive events, or the presence of a high p_T particle may be indicative of a hot spot in the medium. Imperfect correlations between the $n = 2$ and higher order reaction planes [43], possibly due to a difference between the reaction plane for flow and jet quenching [44], would reduce the \tilde{v}_n^t and increase \tilde{v}_n^a but the RPF method would still provide a valid description of the background. The fit parameters in Table I therefore should not be considered a measurement of the v_n due to flow. While the RPF method assumes that the large $\Delta\eta$ correlation function on the near-side contains no signal, no assumptions are made about the event sample and the background is weighted correctly over background pairs by construction. The background determined using the RPF method is therefore more robust than that determined using the ZYAM method.

Background subtracted di-hadron correlations with $4.0 < p_T^t < 6.0$ GeV/c and $1.5 < p_T^a < 4.0$ GeV/c in $d + Au$ and $Au + Au$ collisions at $\sqrt{s_{NN}} = 200$ GeV are shown in Figure 1. Typical uncertainties in Figure 1 are less than the uncertainty due to the background level alone using the ZYAM method and the uncertainty in the near-side in-plane peak region is about one fifth of the uncertainty using ZYAM [40]. The data are inconsistent with the presence of the Mach cone [11, 15–18], indicating that it was an artifact of the background subtraction.

The yield is reported in order to quantitatively compare correlation functions in $Au + Au$ collisions to $d + Au$ collisions. The yield is calculated as

$$Y = \int_a^b \frac{1}{N_t} \frac{dN}{d\Delta\phi} d\Delta\phi \quad (2)$$

where the integration limits $a = -0.79$ and $b = 0.79$ on the near-side and $a = 2.36$ and $b = 3.93$ on the away-side are chosen to match the binning in the STAR data. The near-side yield is given in Figure 2(a) and the away-side yield in Figure 2(b). These results have substantially smaller uncertainties than results using the ZYAM method [45]. The yield is highest for the lowest momenta. The near-side yields in $Au + Au$ collisions are within error

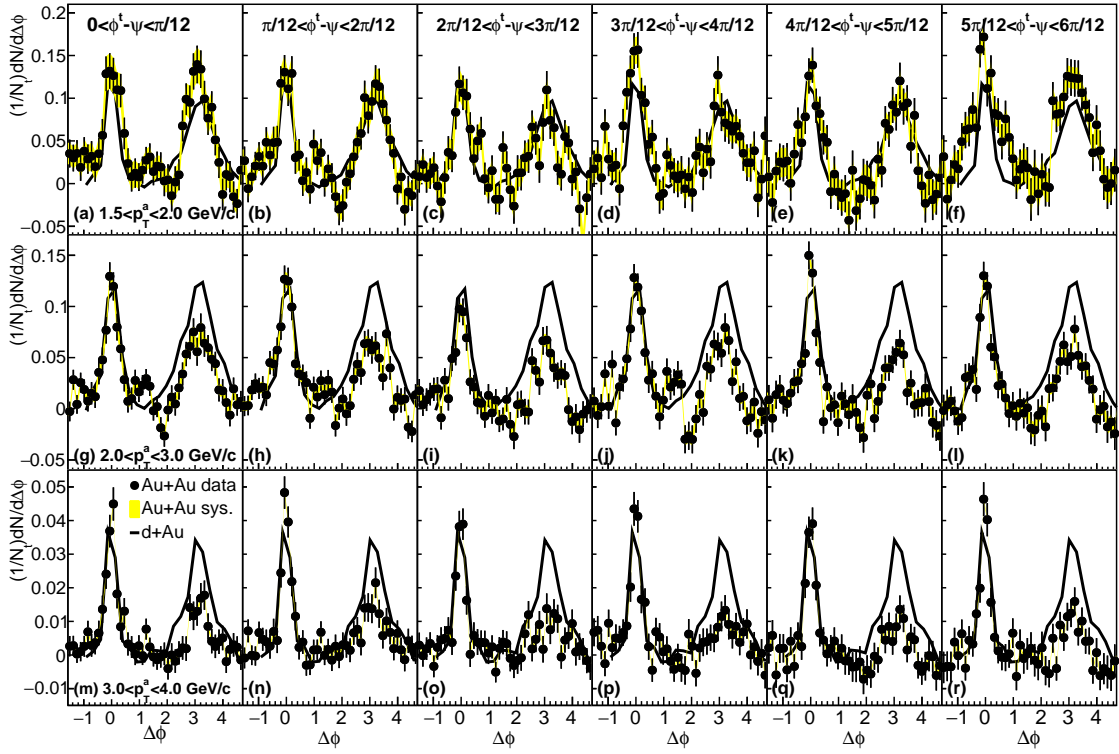


FIG. 1: Background subtracted di-hadron correlations with $4.0 < p_T^t < 6.0$ GeV/c for $1.5 < p_T^a < 2.0$ GeV/c (a-f), $2.0 < p_T^a < 3.0$ GeV/c (g-l), $3.0 < p_T^a < 4.0$ GeV/c (m-r) in $d + Au$ and $Au + Au$ collisions at $\sqrt{s_{NN}} = 200$ GeV for trigger particles from $0 < \phi_s < \pi/12$ (a,g,m), $\pi/12 < \phi_s < 2\pi/12$ (b,h,n), $2\pi/12 < \phi_s < 3\pi/12$ (c,i,o), $3\pi/12 < \phi_s < 4\pi/12$ (d,j,p), $4\pi/12 < \phi_s < 5\pi/12$ (e,k,q), and $5\pi/12 < \phi_s < 6\pi/12$ (f,l,r). Yellow band shows scale uncertainty on $Au + Au$ data. Uncertainty due to reaction plane resolution is not shown but is negligible. The statistical uncertainties on the $Au + Au$ data include uncertainties due to the background determined by the fit in the RPF method and are therefore non-trivially correlated point-to-point.

TABLE I: Fit parameters from RPF method. The $v_2(\%)$ from [40] are listed for comparison to $\tilde{v}_2^a(\%)$. For $4.0 < p_T < 6.0$ GeV/c $v_2 = 16.3 \pm 2.0$ from [40].

p_T^a (GeV/c)	χ^2/NDF	B	$v_2(\%)$ from [40]	$\tilde{v}_2^a(\%)$	$\tilde{v}_2^t(\%)$	$\tilde{v}_3^t \tilde{v}_3^a (\times 10^{-4})$	$\tilde{v}_4^a(\%)$	$\tilde{v}_4^t(\%)$
1.5–2.0	1.00	0.7 ± 0.0	16.4 ± 1.1	18.1 ± 0.2	9.3 ± 1.6	109 ± 17	2.6 ± 0.4	0.10 ± 0.08
2.0–3.0	1.23	0.3 ± 0.0	18.9 ± 1.2	20.7 ± 0.3	8.7 ± 2.4	159 ± 28	4.4 ± 0.7	0.10 ± 0.08
3.0–4.0	1.04	0.0 ± 0.0	19.4 ± 1.3	22.9 ± 1.0	10.8 ± 7.0	190 ± 89	2.7 ± 2.1	0.10 ± 0.07

of the yields in $d + Au$ collisions but the away-side yields are below those in $d + Au$ collisions.

I_{AA} has been used to quantify the suppression observed in di-hadron correlations [46], analogous to measurements of the nuclear modification factor. We calculate I_{AA} as

$$I_{AA} = Y_{Au+Au}/Y_{d+Au}. \quad (3)$$

Note that equation 3 differs from the standard definition of I_{AA} , which has the yield from $p+p$ collisions in the denominator. No differences have been observed between di-hadron correlations in $p+p$ and $d + Au$ [47] and only $d + Au$ data are available in [40]. The near-side I_{AA} is given in Figure 2(c) and the away-side I_{AA} in Figure 2(d). The near-side I_{AA} is within error of 1.0 with little reaction plane dependence, although I_{AA} is

also consistent with the slight enhancement observed at the LHC [48]. The away-side I_{AA} is around 0.3 for $3.0 < p_T^a < 4.0$ GeV/c, increasing with increasing p_T^a . The higher I_{AA} for lower p_T^a is consistent with the softening of the fragmentation function expected in response to the medium. I_{AA} is highest both in- and out-of-plane for $1.5 < p_T^a < 2.0$ GeV/c. A similar trend is indicated for $2.0 < p_T^a < 3.0$ GeV/c, although with less significance. Correlations with a trigger out-of-plane may be more surface biased than those in-plane and therefore less modified, or they may interact with more medium. The reaction plane dependence observed may be due to an interplay between these effects.

Early results demonstrated a complete suppression of the away-side in central collisions [10], a highly cited and influential result. The I_{AA} in [10] is consistent within the

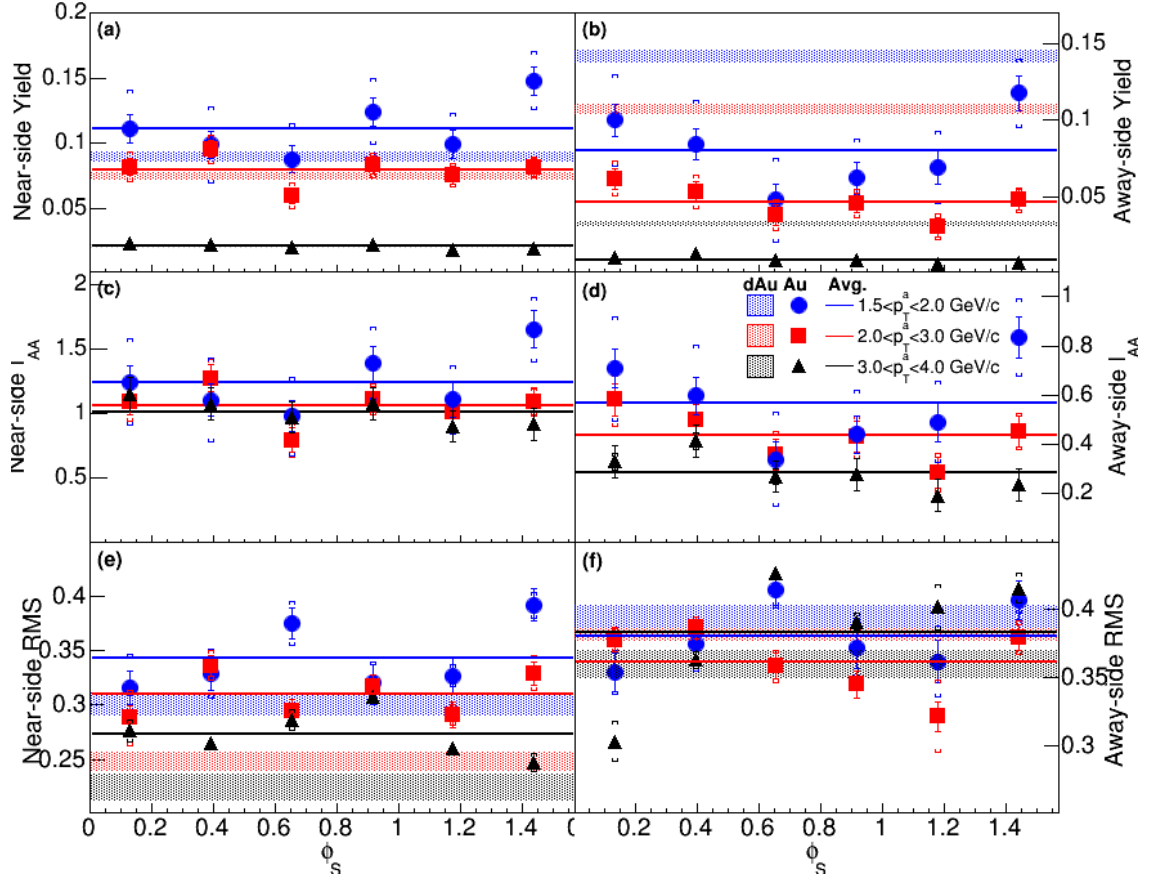


FIG. 2: Yields (a,b), truncated RMS (c,d), and I_{AA} (e,f) for the near-side (a,c,e) and away-side (b,d,f). Systematic uncertainties are 100% correlated point to point. Statistical uncertainties are non-trivially correlated point to point for a fixed p_T^a but are uncorrelated for different p_T^a . Lines show the average for all ϕ_s and bands show the value for $d + Au$ collisions with the width representing the error bar.

large uncertainties with Figure 2(a) and Figure 2(b) for the same centralities. However, since we observe qualitatively different results from studies using the same methodology [11, 15–18], the complete suppression of the away-side in [10] is likely also an artifact of the background subtraction.

We also report the truncated RMS

$$RMS = \sqrt{\int_a^b \frac{1}{Y N_t} \frac{dN}{d\Delta\phi} (\Delta\phi - \Delta\phi_0)^2 d\Delta\phi} \quad (4)$$

where $\Delta\phi_0 = 0$ for the near-side and π for the away-side rather than the RMS over all $\Delta\phi$ because integration over a wide range in $\Delta\phi$ increases the weight of statistical error bars without dramatically changing the result. The integration limits are the same as for equation 2. The near-side RMS is given in Figure 2(e) and the away-side RMS in Figure 2(f). The near-side RMS is larger than the $d + Au$ RMS for the same p_T^a for all ranges of p_T^a studied. Such broadening is consistent with expectations from energy loss through either bremsstrahlung or collisional energy loss, since the energy would remain spatially correlated with the parent parton but be dis-

tributed over a somewhat wider area [49]. This indicates that the near-side is modified even though the yields are consistent with those in $d + Au$ collisions, consistent with observations in [12]. There is little indication of ϕ_s -dependent modifications on the near-side. The away-side RMS in $Au + Au$ collisions is mostly consistent with that in $d + Au$ collisions. Since broadening is apparent on the near-side, this may indicate that the away-side RMS is less sensitive to observation of broadening because the away-side is already broader than the near-side, even in $d + Au$ collisions, due to the difference between the trigger particle's angle and the angle of the away-side jet.

These high precision results are consistent with the modification of fragmentation functions in $Pb + Pb$ collisions observed at the LHC, which indicated broadening and softening of the fragmentation function [20, 21]. This demonstrates the efficacy of the RPF method for precision studies of di-hadron and jet-hadron correlations, particularly at low momenta.

III. CONCLUSIONS

The effects observed in di-hadron correlations relative to the reaction plane using the RPF method indicate that medium-induced modifications to jet-like correlations are more subtle than earlier results using the ZYAM method and neglecting odd v_n . This indicates that jets do not equilibrate fully with the medium but lost energy remains spatially correlated with the parent parton and that the complete suppression observed in [10] was likely also an artifact of the background subtraction. These results agree better with results from fully reconstructed jets, which do not indicate dramatic shape modifications or complete equilibration but slight broadening and more subtle modifications of the fragmentation function [20, 21], than with earlier results indicating a dip [11, 15–18], or “Mach cone“, on the away-side.

IV. ACKNOWLEDGEMENTS

We are grateful to Jana Bielčikova, Marco van Leeuwen, Søren Sørensen, and Paul Stankus for useful comments on the manuscript and to Frank Geurts, Fuqiang Wang, and the STAR collaboration for productive communication about the STAR data. This work was supported in part by funding from the Division of Nuclear Physics of the U.S. Department of Energy under Grant No. DE-FG02-96ER40982.

-
- [1] K. Adcox et al. (PHENIX), Nucl. Phys. **A757**, 184 (2005).
 - [2] J. Adams et al. (STAR), Nucl. Phys. **A757**, 102 (2005).
 - [3] B. B. Back et al., Nucl. Phys. **A757**, 28 (2005).
 - [4] I. Arsene et al. (BRAHMS), Nucl. Phys. **A757**, 1 (2005).
 - [5] J. Adams et al. (STAR), Phys. Rev. Lett. **91**, 172302 (2003).
 - [6] S. Adler et al. (PHENIX), Phys. Rev. Lett. **91**, 072301 (2003).
 - [7] B. Back et al. (PHOBOS), Phys. Rev. **C70**, 061901 (2004).
 - [8] K. Aamodt et al. (ALICE), Phys. Lett. **B696**, 30 (2011).
 - [9] S. Chatrchyan et al. (CMS), Eur. Phys. J. **C72**, 1945 (2012).
 - [10] C. Adler et al. (STAR), Phys. Rev. Lett. **90**, 082302 (2003).
 - [11] S. Adler et al. (PHENIX), Phys. Rev. Lett. **97**, 052301 (2006).
 - [12] G. Agakishiev et al. (STAR), Phys. Rev. **C85**, 014903 (2012).
 - [13] B. Abelev et al. (STAR), Phys. Lett. **B683**, 123 (2010).
 - [14] B. Abelev et al. (STAR), Phys. Rev. **C80**, 064912 (2009).
 - [15] A. Adare et al. (PHENIX), Phys. Rev. Lett. **98**, 232302 (2007).
 - [16] A. Adare et al. (PHENIX), Phys. Rev. **C77**, 011901 (2008).
 - [17] B. Abelev et al. (STAR), Phys. Rev. Lett. **102**, 052302 (2009).
 - [18] M. Aggarwal et al. (STAR), Phys. Rev. **C82**, 024912 (2010).
 - [19] G. Torrieri, B. Betz, J. Noronha, and M. Gyulassy, Acta Phys. Polon. **B39**, 3281 (2008).
 - [20] G. Aad et al. (ATLAS), Phys. Lett. **B739**, 320 (2014).
 - [21] S. Chatrchyan et al. (CMS), Phys. Rev. **C90**, 024908 (2014).
 - [22] J. Bielcikova, S. Esumi, K. Filimonov, S. Voloshin, and J. Wurm, Phys. Rev. **C69**, 021901 (2004).
 - [23] J. Adams et al. (STAR), Phys. Rev. Lett. **95**, 152301 (2005).
 - [24] J. Adams et al. (STAR), Phys. Rev. Lett. **97**, 162301 (2006).
 - [25] A. Adare et al. (PHENIX), Phys. Rev. **C78**, 014901 (2008).
 - [26] N. N. Ajitanand, J. M. Alexander, P. Chung, W. G. Holzmann, M. Issah, R. A. Lacey, A. Shevel, A. Taranenko, and P. Danielewicz, Phys. Rev. **C72**, 011902 (2005).
 - [27] P. Sorensen, J. Phys. **G37**, 094011 (2010).
 - [28] B. Alver and G. Roland, Phys. Rev. **C81**, 054905 (2010), [Erratum: Phys. Rev. **C82**, 039903(2010)].
 - [29] K. Aamodt et al. (ALICE), Phys. Rev. Lett. **107**, 032301 (2011).
 - [30] L. Adamczyk et al. (STAR), Phys. Rev. **C88**, 014904 (2013).
 - [31] A. Adare et al. (PHENIX), Phys. Rev. Lett. **107**, 252301 (2011).
 - [32] I. Bouras, A. El, O. Fochler, H. Niemi, Z. Xu, and C. Greiner, Acta Phys. Polon. Supp. **5**, 1143 (2012).
 - [33] I. Bouras, A. El, O. Fochler, H. Niemi, Z. Xu, and C. Greiner, Phys. Lett. **B710**, 641 (2012), [Erratum: Phys. Lett. **B728**, 156(2014)].
 - [34] A. Ayala, I. Dominguez, and M. E. Tejeda-Yeomans, Phys. Rev. **C88**, 025203 (2013).
 - [35] I. Bouras, B. Betz, Z. Xu, and C. Greiner, Phys. Rev. **C90**, 024904 (2014).
 - [36] Y. Tachibana and T. Hirano, Phys. Rev. **C93**, 054907 (2016).
 - [37] A. Adare et al. (PHENIX), Phys. Rev. Lett. **111**, 032301 (2013).
 - [38] H. Agakishiev et al. (STAR), Phys. Rev. **C89**, 041901 (2014).
 - [39] N. Sharma, J. Mazer, M. Stuart, and C. Nattrass, Phys. Rev. **C93**, 044915 (2016).
 - [40] H. Agakishiev et al. (STAR) (2010), 1010.0690.
 - [41] T. Sjostrand, S. Mrenna, and P. Z. Skands, JHEP **0605**, 026 (2006).
 - [42] P. Z. Skands, Phys. Rev. **D82**, 074018 (2010).
 - [43] G. Aad et al. (ATLAS), Phys. Rev. **C90**, 024905 (2014).
 - [44] J. Jia, Phys. Rev. **C87**, 061901 (2013).
 - [45] A. Adare et al. (PHENIX), Phys. Rev. **C84**, 024904 (2011).
 - [46] A. Adare et al. (PHENIX), Phys. Rev. **C78**, 014901 (2008).
 - [47] S. Adler et al. (PHENIX), Phys. Rev. **C73**, 054903 (2006).
 - [48] K. Aamodt et al. (ALICE), Phys. Rev. Lett. **108**, 092301 (2012).
 - [49] U. A. Wiedemann, pp. 521–562 (2010), [Landolt-Bornstein **23**, 521(2010)], 0908.2306.